

## Room temperature WGM resonances in the red spectral range from Ho<sup>3+</sup> activated ZnO micro-spherical cavities

K. Fabitha, F. Nagasaki, Y. Fujiwara, Y. Wakiyama, D. Nakamura, and M. S. Ramachandra Rao

Citation: *Appl. Phys. Lett.* **112**, 262102 (2018); doi: 10.1063/1.5031838

View online: <https://doi.org/10.1063/1.5031838>

View Table of Contents: <http://aip.scitation.org/toc/apl/112/26>

Published by the [American Institute of Physics](#)

---

---

**AIP** | Conference Proceedings

Get **30% off** all  
print proceedings!

Enter Promotion Code **PDF30** at checkout



# Room temperature WGM resonances in the red spectral range from Ho<sup>3+</sup> activated ZnO micro-spherical cavities

K. Fabitha,<sup>1</sup> F. Nagasaki,<sup>2</sup> Y. Fujiwara,<sup>2</sup> Y. Wakiyama,<sup>2</sup> D. Nakamura,<sup>2</sup> and M. S. Ramachandra Rao<sup>1,a)</sup>

<sup>1</sup>Department of Physics, Nano Functional Materials Technology Centre and Materials Science Research Centre, Indian Institute of Technology Madras, Chennai 600036, India

<sup>2</sup>Graduate School of Information Science and Electrical Engineering, Kyushu University, 744 Motoooka, Nishi-ku, Fukuoka 819-0395, Japan

(Received 31 March 2018; accepted 8 June 2018; published online 25 June 2018)

Highly crystalline and smooth 1% Ho<sup>3+</sup> doped ZnO microspheres with diameters ranging from 0.5 to 15  $\mu\text{m}$  were synthesized using laser ablation technique. Near band edge whispering gallery mode (WGM) resonances from Ho:ZnO microspheres with a single oscillation route in the UV range are observed with 355 nm excitation. Apart from the significantly enhanced visible WGM resonances associated with intrinsic oxygen vacancy defects by Ho<sup>3+</sup> doping, the visible range WGM resonances associated with the Ho<sup>3+</sup>  $^5F_5 \rightarrow ^5I_8$  emission at 629–690 nm are also observed with a 488 nm excitation. The WGMs of Ho<sup>3+</sup> f-f emission possess lower threshold and high Q-factor values. Published by AIP Publishing. <https://doi.org/10.1063/1.5031838>

ZnO has been exclusively studied for solid state light sources and detectors in the blue and UV ranges because of the direct band gap  $\sim 3.37$  eV and comparatively higher excitonic binding energy  $\sim 60$  meV.<sup>1,2</sup> ZnO micro/nanostructures show distinct mode confinement routes such as Fabry-Perot (FP) modes and whispering gallery modes (WGMs).<sup>3–7</sup> Apart from the UV emission at  $\sim 380$  nm (free exciton emission), ZnO also possesses a broad emission band centered at  $\sim 530$  nm which is expected to originate from the native oxygen vacancy ( $V_{\text{O}}^-$ ) defects.<sup>1,2</sup> We had achieved the sharp visible Ho<sup>3+</sup> f-f emissions from Ho<sup>3+</sup> doped ZnO (Ho:ZnO) nanoparticles with various Ho ion concentrations in our previous work.<sup>8</sup> The important characteristic of rare earth (RE) ions, where Ho is one of the members, is that they emit very sharp lines and are relatively insensitive to the host materials.<sup>9,10</sup> As shown in Fig. 1, in RE ion doped ZnO when a Zn<sup>2+</sup> ion is replaced with a RE ion, emissions originate from the 4f levels of RE ions which are formed as inter-band states in the forbidden gap of ZnO. Our focus is on the visible range optical properties of Ho<sup>3+</sup> doped ZnO microspheres as schematically shown in Fig. 1. An isotropic structure like sphere has been chosen to avoid the confinement loss happening at the edges in other geometries. Recently, a study on Yb:ZnO microsphere showed enhancement in the ZnO native defect related WGM emissions, but no Yb originated emissions are observed.<sup>11</sup> We have observed WGM resonances in Ho<sup>3+</sup> f-f transitions apart from the ZnO intrinsic emissions. In this study, we present the coupling of the sharp visible f-f emissions of Ho<sup>3+</sup> to WGMs of Ho:ZnO spherical cavity.

Figure 2(a) depicts a schematic diagram of the growth process of microspheres together with the atomic force microscopy (AFM) images in Fig. 2(b) and the scanning electron microscopy (SEM) images in Fig. 2(c). We have followed the previous report to synthesis un-doped and 1% Ho:

ZnO microspheres as it is relatively simpler and yields highly crystalline and smooth microspheres over a large range of sizes.<sup>12</sup> The spheres were grown on quartz substrates by ablating undoped and 1% Ho:ZnO sintered targets in air using a Q-switched Nd:YAG laser beam of  $\lambda = 1064$  nm and  $\tau = 5$  ns at a fluency of  $23 \text{ J cm}^{-2}$  and a repetition rate of 10 Hz. The targets were prepared from sol-gel derived nanoparticle powders, cold pressed (with pressure of 7 tons) as pellets with diameter = 13 mm and sintered at 1100 °C for 12 h. SEM and AFM studies were carried out, respectively, using FEI Quanta 3D and Bruker (Dimension edge) with probe SCM-PIT conducting tip of force constant,  $K = 2.5$  N/m and resonance frequency = 75 kHz. SEM and AFM images show that several microspheres with highly smooth (roughness  $\sim 2$  nm) surfaces and different sizes are formed on the substrate. The diameter of the ZnO spheres is found to vary over a large range  $\sim 0.5$ – $15 \mu\text{m}$ , which has the advantage to explore the lasing properties of individual spheres of different sizes. Average size of the spheres is estimated as  $3 \mu\text{m}$ . The smoothness of the surface is one of the important parameters as whispering gallery modes are waves traveling around the circumference of the resonator due to the total internal reflection, exhibiting sufficiently sharp resonances. Therefore, the rougher surface

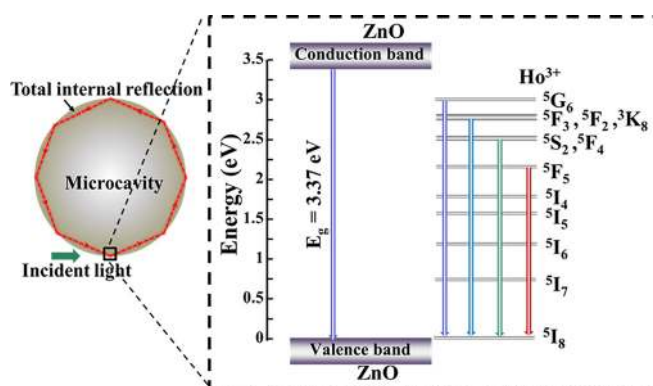


FIG. 1. Energy level diagrams of ZnO and Ho<sup>3+</sup>.

<sup>a)</sup>Electronic mail: msrao@iitm.ac.in

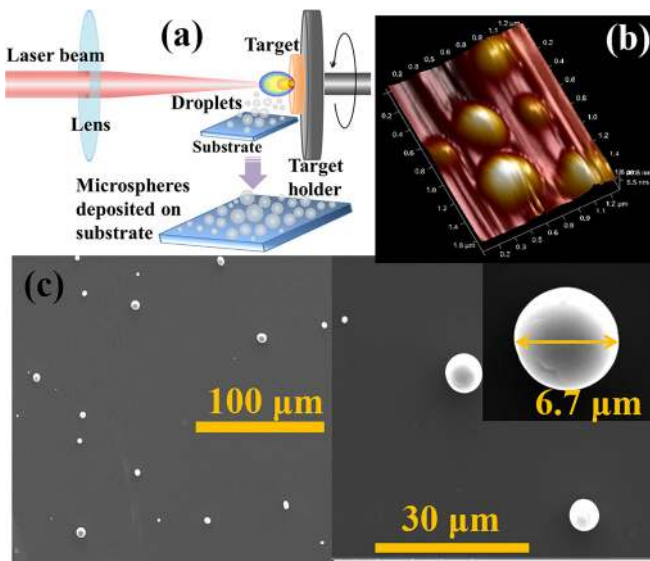


FIG. 2. (a) growth process of microspheres, (b) AFM image of Ho:ZnO microspheres and (c) SEM images of Ho:ZnO microspheres with different magnifications.

causes scattering losses resulting in increased lasing threshold and decreased Q-factor.<sup>13</sup>

Raman spectroscopic measurements were undertaken on individual microspheres by HORIBA Jobin Yvon HR800 UV. Figure 3 represents Raman spectra of undoped and Ho<sup>3+</sup> doped ZnO microspheres of different sizes with the 488 nm line of the Ar<sup>+</sup> laser as excitation source at room temperature. Only the peaks from ZnO are observed. No peaks from any secondary phase are observed although it is challenging to dope larger Ho<sup>3+</sup> (1.015 Å) at Zn<sup>2+</sup> (0.74 Å) site. Because of this size mismatch, the solid solubility limit of Ho<sup>3+</sup> in ZnO is 1 mol. %. We restricted the dopant concentration as 1% by keeping this in mind. It is found that this concentration of Ho<sup>3+</sup> is enough to sustain WGM modes with very decent threshold value and high Q-factor. As shown in Fig. 3, five Raman modes were observed at 96.9 cm<sup>-1</sup>, 332.1 cm<sup>-1</sup>,

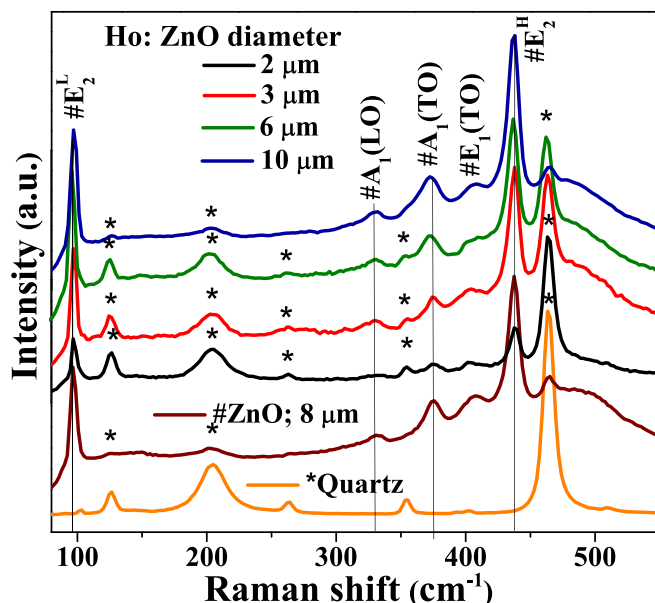


FIG. 3. Micro-Raman spectra from a single Ho:ZnO microsphere with different sizes on quartz substrate.

372.2 cm<sup>-1</sup>, 408.2 cm<sup>-1</sup>, and 437.8 cm<sup>-1</sup>. Raman peaks at 437 cm<sup>-1</sup> and 96 cm<sup>-1</sup> can be assigned to the ZnO non-polar optical phonon E<sub>2</sub><sup>H</sup> and E<sub>2</sub><sup>L</sup> modes, respectively, while the small phonon peaks at 332 cm<sup>-1</sup>, 372 cm<sup>-1</sup>, and 408.2 cm<sup>-1</sup> can be attributed to E<sub>2</sub><sup>H</sup>–E<sub>2</sub><sup>L</sup> probably marking multi-phonon scattering, A<sub>1</sub>(TO) and E<sub>1</sub>(TO) modes, respectively.<sup>14–16</sup> The strong phonon peak at 437 cm<sup>-1</sup>, known as the signature peak of wurtzite structure of ZnO, confirms that the spheres crystallize in hexagonal wurtzite ZnO structure with high crystalline quality, which is consistent with previous reports.<sup>12,17,18</sup> The peaks at 126.5 cm<sup>-1</sup>, 204.9 cm<sup>-1</sup>, 262.1 cm<sup>-1</sup>, 353.2 cm<sup>-1</sup>, 401.8 cm<sup>-1</sup>, and 465.4 cm<sup>-1</sup> are Raman modes of quartz, the substrate on which microspheres are deposited.

Figures 4(a) and 4(b) show room temperature PL spectra of single Ho:ZnO microsphere with an approximate diameter,  $2a = 2.5 \mu\text{m}$  and  $6 \mu\text{m}$ , respectively, excited by the third harmonic of a Q-switched Nd:YAG laser beam (New Wave, Polaris II) ( $\lambda = 355 \text{ nm}$ , 5 ns). The observed UV luminescence is attributed to the room temperature free-excitons near the band-edge of ZnO. The absorption of excitation wavelength through the bandgap of ZnO microsphere is coupled to the WGMs of the resonator, resulting in periodic sharp resonance peaks in the PL spectra. The observed peak shift towards the lower energy side from the typical value around 382 nm is also reported in undoped ZnO microspheres.<sup>12,13</sup> In contrast to the report on undoped ZnO microspheres where two modal structures are observed,<sup>12</sup> here only a single modal structure with mode spacing,  $\Delta\lambda = 4.3 \text{ nm}$  and  $2.1 \text{ nm}$  is observed for spheres with  $2a = 2.5 \mu\text{m}$  and  $6 \mu\text{m}$ , respectively. The Q-factor =  $\lambda / \Delta\lambda_{FWHM} = 540$  and  $929.9$  for  $2a = 2.5 \mu\text{m}$  and  $6 \mu\text{m}$ , where  $\lambda = 398.58 \text{ nm}$  and  $398.39 \text{ nm}$ , respectively, which are found to be better values compared to the undoped ZnO microspheres.<sup>12</sup> The high quality factor (Q) shows better light confinement with Ho<sup>3+</sup> doping compared to the undoped ZnO. From Fig. 4(c), the lasing threshold of Ho:ZnO sphere of  $2a = 2.5 \mu\text{m}$  is 850 kW cm<sup>-2</sup> whereas the sphere of  $2a = 6 \mu\text{m}$  is found to be lasing above 465 kW cm<sup>-2</sup>, half of the above threshold because of the better light confinement in the increased volume.

We used asymptotic expansion of the size parameter,  $x_l^i (= 2\pi an/\lambda)$  to assign WGM numbers to the resonance peaks appeared in the micro-PL spectra<sup>19–23</sup>

$$nx_l^i = \nu + 2^{-1/3}\alpha_i\nu^{1/3} - \frac{P}{(n^2 - 1)^{1/2}} + \left(\frac{3}{10 \times 2^{2/3}}\right)\alpha_i^2\nu^{-1/3} - \frac{P\left(n^2 - \frac{2P^2}{3}\right)}{2^{1/3}(n^2 - 1)^{3/2}}\alpha_i\nu^{-2/3} + O(\nu^{-1}),$$

where  $\nu = l + 1/2$ ,  $l$  and  $i$  are angular and radial mode number,  $\alpha_i$  is the  $i^{\text{th}}$  zero of the Airy function,  $n$  is the refractive index of the resonator medium and  $P = n$  for transverse electric (TE) modes and  $1/n$  for transverse magnetic (TM) modes. The angular mode numbers ( $l$ ) of TE modes indicated in Figs. 4(a) and 4(b) were calculated by considering only first radial order ( $i = 1$ ) and refractive index  $n = 2.3$  (assuming no significant change in  $n$  by 1% Ho doping).<sup>24</sup> TM modes possess higher threshold value and would not be able to onset at the given power along with the prominent TE modes.<sup>25</sup> Also TM polarization modes are much weaker

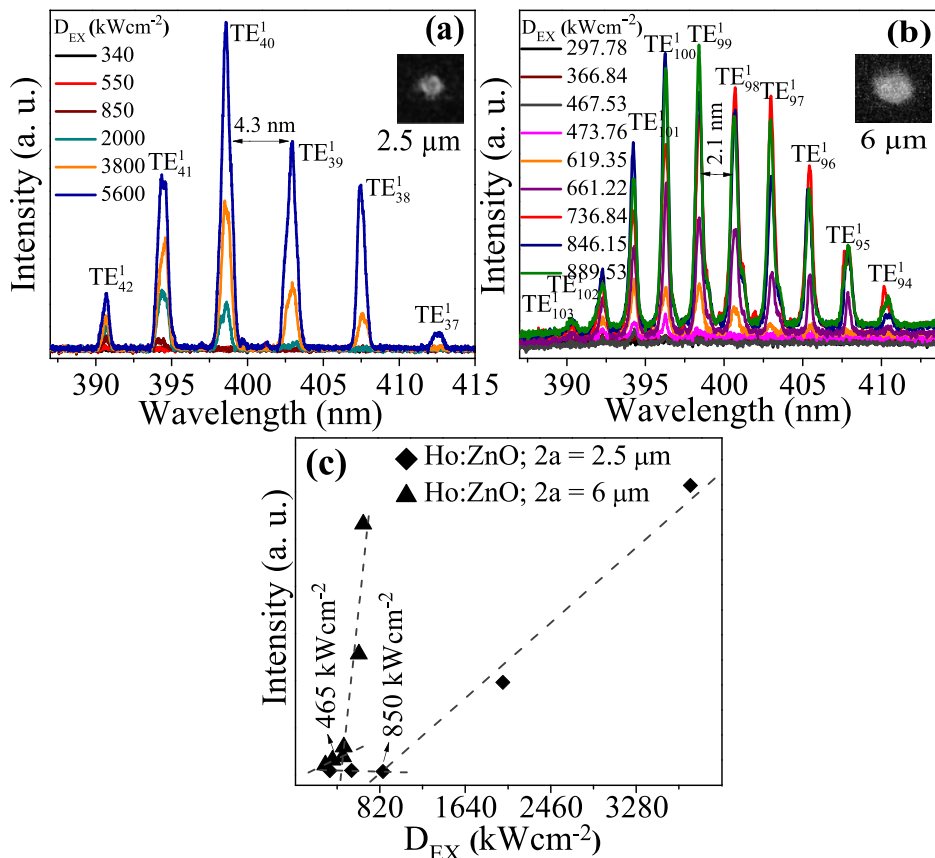


FIG. 4. Room temperature micro-PL spectra pumped with  $\lambda_{ex} = 355$  nm from a single Ho:ZnO microsphere of (a)  $2a = 2.5$   $\mu\text{m}$  and (b)  $2a = 6$   $\mu\text{m}$  at different pumping powers and (c) intensity vs  $D_{EX}$  of peak at 398.58 nm for sphere with  $2a = 2.5$   $\mu\text{m}$  and peak at 398.39 nm for sphere with  $2a = 6$   $\mu\text{m}$ .

than TE modes in UV emission region.<sup>26</sup> This could be the reason why TM modes are not clearly seen in this region. Similar observations are shown in other reports as well.<sup>12,26–28</sup>

The room temperature lasing characteristics in the visible range from single Ho:ZnO spheres, having different sizes were investigated by micro-PL measurements with 488 nm line of Ar<sup>+</sup> laser as the excitation source in the HORIBA Jobin Yvon HR800 UV micro-PL set up. The resultant visible PL spectra are shown in Fig. 5. Intense red luminescence at 629–690 nm from Ho:ZnO spheres is caused by absorption of the excitation wavelength through the 4f levels,  $^5F_5 \rightarrow ^5I_8$  of Ho<sup>3+</sup> which are formed as the inter-band states in the forbidden gap of ZnO. In addition, there is a broad green luminescence at  $\sim 520$ –629 nm associated with recombination of delocalized electrons at singly ionized oxygen vacancies ( $V_{\bar{O}}$ ) with deep trapped holes, observed in undoped ZnO as well. It is observed that the above emissions do not couple to the WGMs in Ho:ZnO microsphere of  $2a = 1$   $\mu\text{m}$  which could be due to the lack of effective confinement within a smaller volume. However, in larger spheres the coupling of Ho<sup>3+</sup>  $^5F_5 \rightarrow ^5I_8$  as well as the native defect emission with the WGMs of Ho:ZnO is effective. This results in periodic sharp resonance peaks of WGM in the visible range of PL spectra as observed in Ho:ZnO microspheres of  $2a = 2$   $\mu\text{m}$ , 6  $\mu\text{m}$ , and 10  $\mu\text{m}$  in Fig. 5(a). In Fig. 5(b), magnified PL spectra in the range of 520–629 nm from undoped ZnO and Ho:ZnO with  $2a = 2$   $\mu\text{m}$  are shown. There is a significant enhancement in the intrinsic defect associated WGMs from Ho:ZnO microspheres compared to the undoped ZnO microspheres as observed in Yb:ZnO microspheres.<sup>11</sup> When Ho<sup>3+</sup> substitutes Zn<sup>2+</sup>, there will be extra electrons and for this

charge compensation  $V_{\bar{O}}$  will be created. Then, enhancement in the luminescence may result from creating more numbers of the electron-hole pairs associated with these increased oxygen vacancies. In addition, Ho<sup>3+</sup> ions may occupy interstitial sites in ZnO, which generate an enormous number of electron trapping centers resulting in increased photoemission process through electron-hole recombination.<sup>29,30</sup>

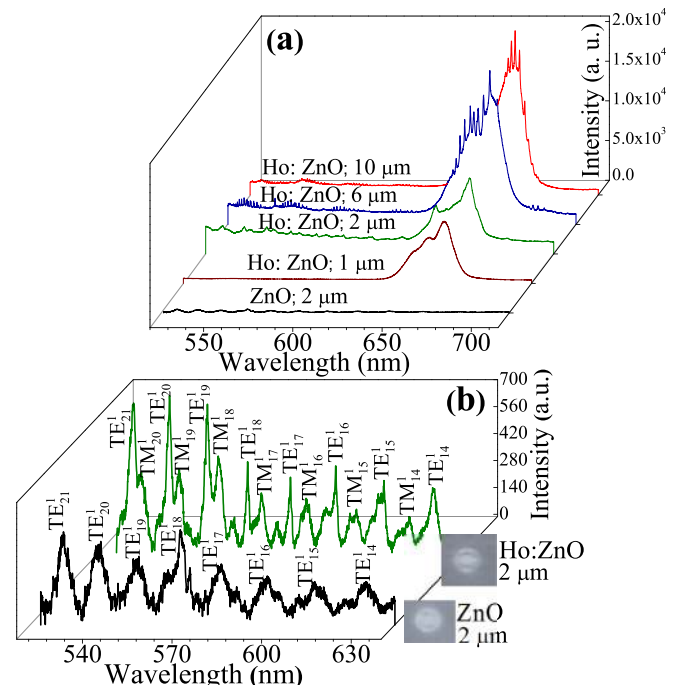


FIG. 5. (a) Room temperature micro-PL spectra with  $\lambda_{ex} = 488$  nm from single Ho:ZnO of different diameters and (b) magnified PL spectra of (a) in the range 520–629 nm of ZnO and Ho:ZnO of  $2a = 2$   $\mu\text{m}$ .

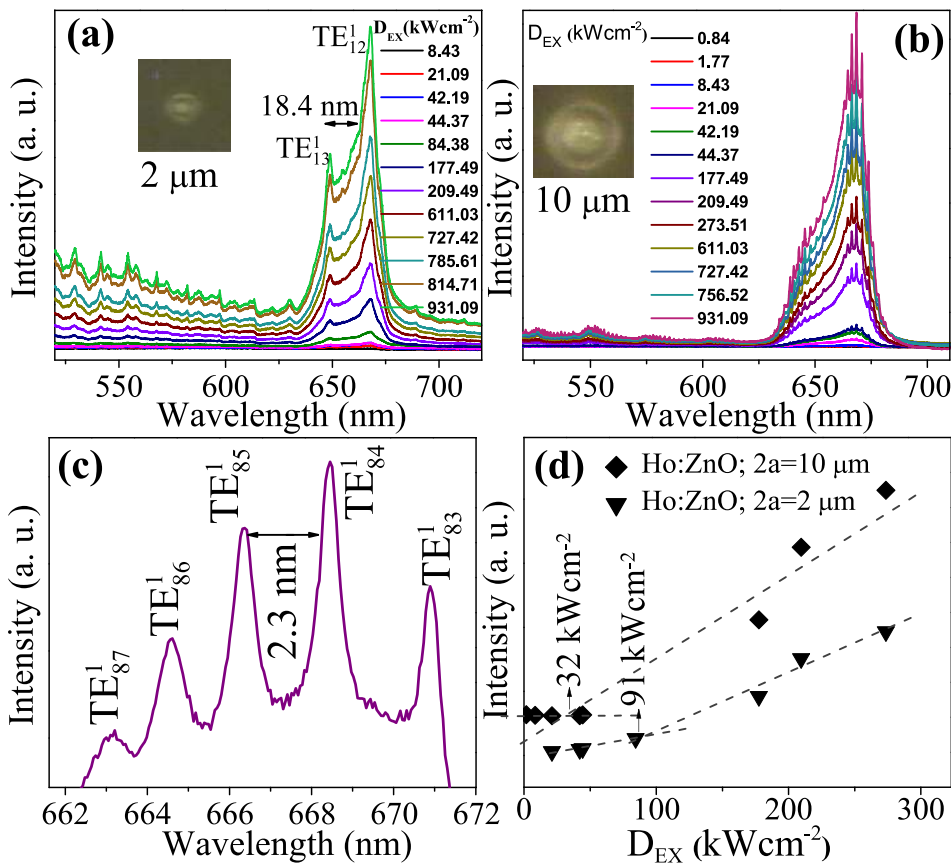


FIG. 6. (a) Room temperature micro-PL spectra with  $\lambda_{ex} = 488$  nm from a single Ho:ZnO microsphere of  $2a = 2 \mu\text{m}$  and (b)  $2a = 10 \mu\text{m}$  at different pumping powers, (c) the magnified region 662–672 nm of (b) with  $D_{EX} = 931 \text{ kW cm}^{-2}$  and (d) intensity vs  $D_{EX}$  of peak at 667.48 nm for sphere with  $2a = 2 \mu\text{m}$  and peak at 668.43 nm for sphere with  $2a = 10 \mu\text{m}$ .

We have examined the lasing threshold of WGM resonances of  $\text{Ho}^{3+} {}^5\text{F}_5 \rightarrow {}^5\text{I}_8$  transition from a single Ho:ZnO microsphere with diameter,  $2a = 2 \mu\text{m}$  and  $10 \mu\text{m}$  by varying the excitation power as shown Figs. 6(a) and 6(b), respectively. The lasing threshold obtained from Fig. 6(d) of Ho:ZnO sphere of  $2a = 2 \mu\text{m}$  is  $91 \text{ kW cm}^{-2}$  whereas the sphere of  $2a = 10 \mu\text{m}$  is found to be lasing above  $32 \text{ kW cm}^{-2}$  because of the better light confinement in the increased volume. Interestingly, these room temperature threshold values are much lower compared to that of near band edge emission. This could be due to the fact that  $\text{Ho}^{3+}$  f-f emissions are more stable and stronger which are unique characteristics of all rare earths. The TE/TM mode numbers are calculated using the above asymptotic expansion with  $n = 1.98$  and are shown in Figs. 5(b), 6(a), and 6(c).<sup>24</sup> In Fig. 5(b), the Ho:ZnO microsphere shows broad and less intense TM modes along with the TE modes. In the case of undoped ZnO microsphere, these modes are very feeble and not able to resolve the TM modes clearly. Therefore, TM modes are not indicated for undoped ZnO microsphere. The TE (both in undoped and Ho:ZnO) and TM modes (in Ho:ZnO) are not showing lasing action and at  $931 \text{ kW cm}^{-2}$  both TE and TM modes are visible. Similar results are reported in the following papers.<sup>11,31</sup> Figures 6(a) and 6(c) do not show TM modes in 629–690 nm region because the threshold for these modes are higher similar to Figs. 4(a) and 4(b). Also, as the TM modes are weaker and have higher line width, these modes could not be resolvable within the background spectrum in this region even if small and broad TM modes are present. Therefore, we think it is reasonable to denote the TE modes in order to discuss the lasing behavior in the case of Figs. 4(a), 4(b), and 6(a)–6(c). In the case of  $\text{Ho}^{3+} {}^5\text{F}_5 \rightarrow {}^5\text{I}_8$

emission, the Q-factor  $= \lambda/\Delta\lambda_{FWHM} = 445$  and  $1155$  for  $2a = 2 \mu\text{m}$  and  $10 \mu\text{m}$  where,  $\lambda_m = 667.48 \text{ nm}$  and  $668.43 \text{ nm}$ , respectively.

In conclusion, highly crystalline and smooth 1%  $\text{Ho}^{3+}$  doped ZnO (Ho:ZnO) micro-spheres with diameters ranging from  $0.5$  to  $15 \mu\text{m}$  were synthesized using simple laser ablation technique. Near band edge WGM resonances from Ho:ZnO micro-spheres with single oscillation route in the UV range are observed with  $355 \text{ nm}$  excitation. The lasing threshold and Q factor are found to be improved compared to that in undoped ZnO. With  $488 \text{ nm}$  excitation, significantly enhanced visible WGM resonances associated with intrinsic oxygen vacancy defects by  $\text{Ho}^{3+}$  doping in Ho:ZnO compared to undoped ZnO have been obtained. Most importantly the visible range WGM resonances in the  $\text{Ho}^{3+} {}^5\text{F}_5 \rightarrow {}^5\text{I}_8$  emission at  $629$ – $690 \text{ nm}$  are also observed with a  $488 \text{ nm}$  excitation with very low threshold and high Q values. These results are promising for ZnO based low power light emitting devices in the visible spectral range. As the WGMs are said to be highly sensitive to the external environments, Ho:ZnO micro-cavities can be used for sensing applications operating in the visible range.

We would like to thank Department of Science and Technology (DST), New Delhi, for the funding that facilitated the Nano Functional Materials Technology Center (Grant No. SRNM/NAT/02-2005). We would also like to thank JSPS and DST under which comes the Japan-India Science Cooperative Program (AJ180083(30-0004-t06)).

<sup>1</sup>H. Morkoç, *Handbook of Nitride Semiconductors and Devices*, Materials Properties, Physics and Growth Vol. 1 (John Wiley & Sons, 2009).

<sup>2</sup>M. R. Rao and T. Okada, *ZnO Nanocrystals and Allied Materials* (Springer, 2013), Vol. 180.

- <sup>3</sup>L. K. Van Vugt, S. Rühle, and D. Vanmaekelbergh, *Nano Lett.* **6**, 2707 (2006).
- <sup>4</sup>K. Okazaki, D. Nakamura, M. Higashihata, P. Iyamperumal, and T. Okada, *Opt. Express* **19**, 20389 (2011).
- <sup>5</sup>G. Zhu, C. Xu, J. Zhu, C. Lv, and Y. Cui, *Appl. Phys. Lett.* **94**, 051106 (2009).
- <sup>6</sup>R. Chen, B. Ling, X. W. Sun, and H. D. Sun, *Adv. Mater.* **23**, 2199 (2011).
- <sup>7</sup>P. J. Pauzauskis, D. J. Sirbulys, and P. Yang, *Phys. Rev. Lett.* **96**, 143903 (2006).
- <sup>8</sup>K. Fabitha and M. R. Rao, *J. Opt. Soc. Am. B* **34**, 2485 (2017).
- <sup>9</sup>S. Cotton, *Lanthanide and Actinide Chemistry* (John Wiley & Sons, 2013).
- <sup>10</sup>K. A. Gschneidner, J.-C. G. Bünzli, and V. K. Pecharsky, *Handbook on the Physics and Chemistry of Rare Earths: Optical Spectroscopy* (Elsevier, 2011), Vol. 37.
- <sup>11</sup>R. Khanum, R. S. Moirangthem, and N. M. Das, *J. Appl. Phys.* **121**, 213101 (2017).
- <sup>12</sup>K. Okazaki, T. Shimogaki, K. Fusazaki, M. Higashihata, D. Nakamura, N. Koshizaki, and T. Okada, *Appl. Phys. Lett.* **101**, 211105 (2012).
- <sup>13</sup>R. S. Moirangthem, P.-J. Cheng, P. C.-H. Chien, B. T. H. Ngo, S.-W. Chang, C.-H. Tien, and Y.-C. Chang, *Opt. Express* **21**, 3010 (2013).
- <sup>14</sup>Y. Lu, H. Ni, Z. Mai, and Z. Ren, *J. Appl. Phys.* **88**, 498 (2000).
- <sup>15</sup>N. Ashkenov, B. Mbenkum, C. Bundesmann, V. Riede, M. Lorenz, D. Spemann, E. Kaidashev, A. Kasic, M. Schubert, and M. Grundmann, *J. Appl. Phys.* **93**, 126 (2003).
- <sup>16</sup>Y. Yang, C. Wang, B. Wang, Z. Li, J. Chen, D. Chen, N. Xu, G. Yang, and J. Xu, *Appl. Phys. Lett.* **87**, 183109 (2005).
- <sup>17</sup>N. Tetsuyama, K. Fusazaki, Y. Mizokami, T. Shimogaki, M. Higashihata, D. Nakamura, and T. Okada, *Opt. Express* **22**, 10026 (2014).
- <sup>18</sup>S. Okamoto, K. Inaba, T. Iida, H. Ishihara, S. Ichikawa, and M. Ashida, *Sci. Rep.* **4**, 5186 (2014).
- <sup>19</sup>C. Lam, P. T. Leung, and K. Young, *J. Opt. Soc. Am. B* **9**, 1585 (1992).
- <sup>20</sup>M. Himmelhaus, S. Krishnamoorthy, and A. Francois, *Sensors* **10**, 6257 (2010).
- <sup>21</sup>A. Francois and M. Himmelhaus, *Sensors* **9**, 6836 (2009).
- <sup>22</sup>S. Pang, R. E. Beckham, and K. E. Meissner, *Appl. Phys. Lett.* **92**, 221108 (2008).
- <sup>23</sup>A. Weller, F. Liu, R. Dahint, and M. Himmelhaus, *Appl. Phys. B* **90**, 561 (2008).
- <sup>24</sup>S. Adachi, *Optical Constants of Crystalline and Amorphous Semiconductors: Numerical Data and Graphical Information* (Springer Science & Business Media, 1999).
- <sup>25</sup>V. D. Ta, R. Chen, and H. D. Sun, *Sci. Rep.* **3**, 1362 (2013).
- <sup>26</sup>J. Dai, C. Xu, P. Wu, J. Guo, Z. Li, and Z. Shi, *Appl. Phys. Lett.* **97**, 011101 (2010).
- <sup>27</sup>J. Dai, C. Xu, K. Zheng, C. Lv, and Y. Cui, *Appl. Phys. Lett.* **95**, 241110 (2009).
- <sup>28</sup>C. Czekalla, C. Sturm, R. Schmidt-Grund, B. Cao, M. Lorenz, and M. Grundmann, *Appl. Phys. Lett.* **92**, 241102 (2008).
- <sup>29</sup>F. Li, X.-C. Liu, R.-W. Zhou, H.-M. Chen, S.-Y. Zhuo, and E.-W. Shi, *J. Appl. Phys.* **116**, 243910 (2014).
- <sup>30</sup>A. Janotti and C. G. Van de Walle, *Phys. Rev. B* **76**, 165202 (2007).
- <sup>31</sup>R. S. Moirangthem and A. Erbe, *Appl. Phys. Lett.* **103**, 051108 (2013).